Cleavage of C−C and C−F Bonds by $Xe^{+\bullet}$ and I^+ Ions in Reactions at a Fluorinated Self-Assembled Monolayer Surface: Collision Energy Dependence and Mechanisms

B. Feng, J. Shen, V. Grill, C. Evans, and R. G. Cooks*

Contribution from the Department of Chemistry, Purdue University, West Lafayette, Indiana 47907

Received September 11, 1997

Abstract: Collisions of $Xe^{+\bullet}$ with a fluorinated self-assembled monolayer surface cause C−C and C−F bond cleavage as evidenced by the reactively scattered ions $XeCF_2^{+\bullet}$, $XeCF^+$, and XeF^+. The projectile ion extracts difluorocarbene from the fluorocarbon to form $XeCF_2^{+\bullet}$ in a low-energy reaction, while simple fluorine abstraction also occurs and yields XeF^+ in a higher energy but entropically favored process. The intact trifluoromethyl iodide radical cation, $ICF_3^{+\bullet}$, resulting from simple C−C cleavage, is observed as a scattered product when I^+ is chosen as projectile, as are analogous ions $IF^{+\bullet}$, $ICF^{+\bullet}$, and ICF_2^+, resulting from C−F and C−C bond cleavage with concomitant I−F and I−C bond formation. Multiple F-atom abstraction occurs in a single collision evidenced by the product, IF_2^+. Density functional theory calculations confirm that the reactions that lead to XeF^+ and $XeCF^+$ are more endothermic than $XeCF_2^{+\bullet}$ formation. The experimental observations and enthalpy calculations suggest that two reaction pathways contribute to XeF^+ formation: oxidative insertion at low collision energy and formation of a fluoronium ion ($-F^+-$) at high collision energy. The generation of $XeCF_2^{+\bullet}$ products is also accounted for through an oxidative insertion mechanism. Although chemical sputtering, i.e., charge exchange with liberation of fluorocarbon cations from the surface, also occurs even at very low collision energy, it does not appear to contribute to the formation of ion/surface reaction products discussed.

Introduction

Activation of the C−F bond is an important issue in chemistry.[1,2] The C−F bond energy (130 kcal/mol in $F-C_2F_5$) is much higher than that of the C−C bond (97 kcal/mol in CF_3-CF_3) or the C−H bond (98 kcal/mol in $H-C_2H_5$)[3] and fluorocarbons are distinguished by their chemical inertness.[4] Numerous investigations on fluorine and fluorocarbons have shaped an independent area in chemistry,[5] in which C−F bond activation is a core topic.

Low-energy (10−100 eV) ion/surface collisions are of growing interest for the preparation of chemically modified surfaces[6−9] and as a means of uncovering novel chemical processes at interfaces.[10,11] While inelastic collisions which lead to surface-induced dissociation (SID) have been accorded most attention,[12−16] ion/surface reactions are being explored in increasing detail. These chemical reactions occur between the projectile ion, or its fragments, and specific chemical functional groups present on the surface.[17−24] One of the best-studied ion/surface reactions is the protonation or alkylation of incident polyatomic projectiles, especially in the case of such radical cations as the molecular ions of pyrazine[25] and benzene.[11] Alkyl transfer occurs upon collision at a surface bearing hydrocarbons, including hydrocarbon thin films and alkylthiolate self-as-

* To whom correspondence should be addressed.

(1) Burdeniuc, J.; Crabtree, R. H. *Science* **1996**, *271*, 340.
(2) Smart, B. E. *Chem. Rev.* **1996**, *96*, 1555.
(3) Lide, D. R., Ed. *CRC Handbook of Chemistry and Physics*, 75th ed.; CRC Press: Ann Arbor, MI, 1994.
(4) Banks, E.; Barlow, M. G. *Fluorocarbon and Related Chemistry*; Thanet Press: Margate, UK, 1971; Vol. 1.
(5) Banks, R. E.; Sharp, D. W. A.; Tatlow, J. C., Eds. *Fluorine: the First Hundred Years*; Lausanne: New York, 1986.
(6) Pradeep, T.; Feng, B.; Ast, T.; Patrick, J. S.; Cooks, R. G.; Pachuta, S. A. *J. Am. Soc. Mass Spectrom.* **1995**, *6*, 187.
(7) Ada, T. A.; Hanley, L.; Etchin, S.; Melngilis, J.; Dressick, W. J.; Chen, M.-S.; Calvert, J. M. *J. Vac. Sci. Technol. B* **1995**, *13*, 2189.
(8) Kuttel, O. M.; Groening, P.; Agostino, R. G.; Schlapbach, L. *J. Vac. Sci. Technol. A* **1995**, *13*, 2848.
(9) Kasi, S. R.; Kang, H.; Sass, C. S.; Rabalais, J. W. *Surf. Sci. Rep.* **1989**, *10*, 1.
(10) Pradeep, T.; Patrick, J. S.; Feng, B.; Miller, S. A.; Ast, T.; Cooks, R. G. *J. Phys. Chem.* **1995**, *99*, 2941.
(11) Somogyi, A.; Kane, T. E.; Ding, J.-M.; Wysocki, V. H. *J. Am. Chem. Soc.* **1993**, *115*, 5275.
(12) Cooks, R. G.; Ast, T.; Pradeep, T.; Wysocki, V. H. *Acc. Chem. Res.* **1994**, *27*, 316.
(13) Dongre, A. R.; Somogyi, A.; Wysocki, V. H. *J. Mass Spectrom.* **1996**, *31*, 339.
(14) Burroughs, J. A.; Wainhaus, S. B.; Hanley, L. *J. Chem. Phys.* **1995**, *103*, 6706.
(15) Chorush, R. A.; Little, D. P.; Beu, S. C.; Wood, T. D.; McLafferty, F. W. *Anal. Chem.* **1995**, *67*, 1042.
(16) Hayward, M. J.; Park, F. D. S.; Manzella, L. M.; Bernasek, S. L. *Int. J. Mass Spectrom. Ion Processes* **1995**, *148*, 25.
(17) Mabud, M. A.; Ast, T.; Verma, S.; Jiang, Y.-X.; Cooks, R. G. *J. Am. Chem. Soc.* **1987**, *109*, 7597.
(18) Pradeep, T.; Riederer, D. E., Jr.; Hoke, S. H., II; Ast, T.; Cooks, R. G.; Linford, M. R. *J. Am. Chem. Soc.* **1994**, *116*, 8658.
(19) Miller, S. A.; Luo, H.; Jiang, X.; Rohrs, H. W.; Cooks, R. G. *Int. J. Mass Spectrom. Ion Processes* **1997**, *160*, 83.
(20) Hayward, M. J.; Park, F. D. S.; Phelan, L. M.; Bernasek, S. L.; Somogyi, A.; Wysocki, V. H. *J. Am. Chem. Soc.* **1996**, *118*, 8375.
(21) Kane, T. E.; Wysocki, V. H. *Int. J. Mass. Spectrom. Ion Processes* **1994**, *140*, 177.
(22) Williams, E. R.; Jones, G. C., Jr.; Fang, L.; Zare, R. N.; Garrison, B. J.; Brenner, D. W. *J. Am. Chem. Soc.* **1992**, *114*, 3207.
(23) Yang, M. C.; Lee, H. W.; Kang, H. *J. Chem. Phys.* **1995**, *103*, 5149.
(24) Beck, R. D.; St. John, P.; Alvarez, M. M.; Diederich, F.; Whetten, R. L. *J. Phys. Chem.* **1991**, *95*, 8402.
(25) Winger, B. E.; Julian, R. J., Jr.; Cooks, R. G.; Chidsey, C. E. D. *J. Am. Chem. Soc.* **1991**, *113*, 8967.

S0002-7863(97)03201-0 CCC: $15.00 © 1998 American Chemical Society
Published on Web 07/24/1998

sembled monolayer (SAM) surfaces.[26] An analogous reaction, atomic fluorine or fluorocarbon group abstraction, is observed when appropriate atomic or polyatomic projectile ions collide with fluorinated SAM surfaces.[11,27−29]

Self-assembled monolayer surfaces are particularly useful as targets for investigations of ion/surface collisions. Fluorinated SAM (F-SAM) surfaces, in particular, are (i) virtually free of adventitious hydrocarbons under relatively modest (10^{-8} Torr) vacuum conditions, (ii) show a small degree of neutralization of the projectile ion (the ionization energy for C_3F_8 is 13.38 eV while that for C_3H_8 is 10.95 eV),[30] and (iii) display very effective translational to internal energy transfer (T → V conversion factor is ca. 20%).[31,32]

In studies of ion/surface reactions at low collision energy, three issues are of general concern: (i) the scope of this field of chemistry, especially the possible existence of new reaction types, (ii) the energetics of the ion/surface reactions, and (iii) their reaction mechanisms and dynamics. The first interest is being pursued in this and other laboratories by examining a wide variety of reagent ions. Comparisons of experimental data for surface reactions with those for analogous ion/molecule reactions is also a valuable means of discovering and understanding ion/surface reactivity.[11,20,27,28,33,34] Progress has been made on the second issue by examining reactions as a function of collision energy and utilizing experimental data from the corresponding gas-phase reactions[30,35] or using theoretical calculations[11,20] to estimate reaction exo- or endothermicities. Molecular dynamics simulations have also been used to study ion/surface reaction processes, and the results suggest that at least some reactions occur on the femto- to picosecond time scale.[22,36] Many observed ion/surface reactions are exothermic, but endothermic reactions are also common and appear to be driven by using the collision energy to overcome the thermochemical barrier.[9,27,28,31,37] For example, collision of $CH_4^{+\bullet}$ with an F-SAM surface does not yield peaks corresponding to CH_nF^+ ($n = 0-2$) at 20 eV collision energy, but these reaction products are abundant at 50 eV collision energy.[28] Thermochemically, the formation of CH_nF^+ products as a result of $CH_4^{+\bullet}$ collisions with an F-SAM surface is estimated to be 108, 95, and 36 kcal/mol endothermic, for $n = 0$, 1, and 2, respectively.[30] The increase in collision energy to 50 eV facilitates these endothermic reactions.

The dependence of ion/surface reactions on collision energy invites comparison with the more thoroughly characterized translational to internal energy (T → V) conversion during inelastic ion/surface collisions.[31,32] Previous studies for several systems showed that roughly 20% of the laboratory translational energy of the projectile is converted into internal energy in the course of inelastic collisions with an F-SAM surface, and this energy then leads to dissociation of the projectile.[28,31,32] The efficiency of energy conversion depends on the type of surface used.[24,30,32,38] By varying the surface impact energy, the internal energy deposited into the projectile ion can be finely controlled and a breakdown curve for the ion—i.e., the internal energy dependence of its fragmentation—can be recorded.[32,39,40] A recent example is provided by the distinction in this fashion between isomeric $C_3H_4^{+\bullet}$ ions.[32] In contrast to the situation for inelastic collisions, just described, very little is known about the conversion from translational energy into internal energy in the course of ion/surface reactive collisions.

Turning to the third issue, the question of ion/surface reaction mechanisms, one notes that at least four pathways have been proposed to account for observed ion/surface reactions. They are distinguished mainly by whether charge transfer is involved. In the charge-transfer mechanism, the incoming projectile ion undergoes charge exchange with the surface functional group producing a surface-bound radical cation. Fragment ions arising from this species are attached to the neutralized projectile in a subsequent ion/molecule reaction at the interface.[11,22,25] This reaction pathway is believed to be responsible for hydrogen atom and alkyl group abstraction by aromatic and heteroaromatic radical cations. This includes attachment of CH_3 (from hydrocarbon surfaces) to the molecular ions of pyrazine[25] yielding methylated pyrazine, as well as CH_n to C_6H_n ($n = 1-3$) pickup by naphthalene molecular ions.[22] Formation of $C_7H_7^+$ from low-energy collisions of the benzene molecular ion at a hydrocarbon-covered surface has similarly been suggested to occur by recombination of a charge-transfer product ion, such as CH_3^+ and $C_2H_5^+$, with the neutralized projectile.[20] Abstraction of multiple hydrogen atoms by pyrazine and pyrene molecular ions from H-SAMs is known to occur from the same carbon chain, but the mechanism of this variant on the reaction is not known.[41]

A second ion/surface reaction mechanism exists which does not involve charge exchange between the surface and the projectile ion. Using low-energy Cs^+ ions bombarding various Si(111) surfaces, Kang and co-workers showed that ions such as $CsSi^{+\bullet}$ and CsH_2O^+ were generated via a two-step process occurring without charge exchange. Instead, collision-induced desorption of the neutrals from the surface was followed by a gas-phase ion/molecule reaction.[42−44] Such ion/neutral electrostatic recombination reactions are facilitated by extensive energy loss of the projectile to the surface and the efficient secondary neutral emission which occurs even at low impact energies. A third mechanism, which combines features of the first two, is that in which the projectile reacts with sputtered neutral fragments in a gas-phase reaction. This has been suggested by Bernasek and co-workers[45] as an alternative

(26) Porter, M. D.; Bright, T. B.; Allara, D. L.; Chidsey, C. E. D *J. Am. Chem. Soc.* **1987**, *109*, 3559.
(27) Pradeep, T.; Ast, T.; Cooks, R. G.; Feng, B. *J. Phys. Chem.* **1994**, *98*, 9301.
(28) Ast, T.; Pradeep, T.; Feng, B.; Cooks, R. G. *J. Mass Spectrom.* **1996**, *31*, 791.
(29) Riederer, D. E., Jr.; Miller, S. A.; Ast, T.; Cooks, R. G. *J. Am. Soc. Mass Spectrom.* **1993**, *4*, 938.
(30) Lias, S. G.; Bartmess, J. E.; Liebman, J. F.; Holmes, J. H.; Levin, R. D.; Mallard, W. G. *J. Phys. Chem. Ref. Data* **1988**, 17, Suppl. 1.
(31) Morris, M. R.; Riederer, D. E., Jr.; Winger, B. E.; Cooks, R. G.; Ast, T.; Chidsey, C. E. D. *Int. J. Mass Spectrom. Ion Processes* **1992**, *122*, 181.
(32) Hayakawa, S.; Feng, B.; Cooks, R. G. *Int. J. Mass Spectrom. Ion Processes* **1997**, *167/168*, 525.
(33) Wu, Q.; Hanley, L. *J. Phys. Chem.* **1993**, *97*, 2677.
(34) Kane, T. E.; Somogyi, A.; Wysocki, V. H. *Org. Mass Spectrom.* **1993**, *28*, 1665.
(35) Mallard, W. G., Ed. *NIST World Wide Web Standard Reference Database*, **1997**, http://webbook.nist.gov.
(36) Garrison, B. J.; Kodali, P. B. S.; Srivastava, D. *Chem. Rev.* **1996**, *96*, 1327.
(37) Koppers, W. R.; Beijersbergen, J. H. N.; Tsumori, K.; Weeding, T. L.; Kistemaker, P. G.; Kleyn, A. W. *Surf. Sci.* **1996**, *358*, 678.
(38) Wysocki, V. H.; Ding, J.-M.; Jones, J. L.; Callahan, J. H.; King, F. L. *J. Am. Soc. Mass Spectrom.* **1992**, *3*, 27.
(39) Vekey, K.; Somogyi, A.; Wysocki, V. H. *J. Mass Spectrom.* **1995**, *30*, 212.
(40) Zhong, W.; Nikolaev, E. N.; Futrell, J. H.; Wysocki, V. H. *Anal. Chem.* **1997**, *69*, 2496.
(41) Riederer, D. E., Jr.; Cooks, R. G.; Linford, M. R. *J. Mass Spectrom.* **1995**, *30*, 241.
(42) Yang, M. C.; Lee, H. W.; Kang, H. *J. Chem. Phys.* **1995**, *103*, 5149.
(43) Yang, M. C.; Hwang, C. H.; Ku, J. K.; Kang, H. *Surf. Sci.* **1996**, *366*, L719.
(44) Yang, M. C.; Hwang, C. H.; Kang, H. *J. Chem. Phys.* **1997**, *107*, 2611.
(45) Phelan, L. M.; Hayward, M. J.; Flynn, J. C.; Bernasek, S. L. *J. Am. Chem. Soc.* In press.

explanation for the alkyl transfer reaction to radical cations. The overall thermochemistry of this process is identical to the charge exchange mechanism.

Studies in this laboratory have revealed a fourth mechanism in which ion/surface reaction products are generated by fragmentation of intermediates formed via oxidative addition of the projectile ion, or its SID fragments, to groups present at the F-SAM surface. Some of the reactions which occur by this process are those which result in fluorine atom and fluorocarbon group addition.[6,11,18,19,27,28] The experimental data provide several reasons which suggest that charge exchange is not involved in this type of ion/surface reaction. First, fluorine pick-up occurs at energies below those which lead to chemical sputtering.[46] For a given surface, chemical sputtering depends on the nature and collision energy of the projectile, i.e., its mass and recombination energy, as well as the ionization energy of the surface group. For F-SAM surfaces, $C_nF_m^+$ ions are often observed as chemically sputtered ions.[6,28] Transition metal ions, such as 30 eV $Fe^{+\bullet}$, abstract fluorine atoms from F-SAM surfaces, but no chemical sputtering is observed under these conditions, suggesting that charge exchange is not involved.[18] Second, the difference between the recombination energy of the projectiles and the ionization energy of the surface *need* not favor charge exchange. For example, in multiple fluorine atom abstraction from F-SAM surfaces by transition metals (e.g. TiF_3^+ generated from $Ti^{+\bullet}$, $CrF_2^{+\bullet}$ from $Cr^{+\bullet}$, and WF_5^+ from $W^{+\bullet}$),[18] the recombination energy of the metal ions is lower than that of the surface fluorocarbon group, suggesting that fluorine atom abstraction takes place only from the neutral species and that the process does not require energetically unfavorable ion neutralization before reaction.[18] Furthermore, in Cl-for-F transhalogenation experiments between the F-SAM surface and $SiCl_4^{+\bullet}$ ions, the surface fluorine atom is exchanged with a chlorine atom from the projectile, leaving a ClF_2C- group bound to the surface.[6] This process is most readily explained as the result of atom transfer without charge exchange. Finally, for a different system, when ^{13}C-labeled $^{13}CH_n^+$ projectile ions are reacted with an F-SAM surface, the formation of $^{12}CF^+$ and $^{13}CF^+$ is observed in equal abundance.[28] The results of this study indicate that a symmetrical collision complex, such as a fluoronium ion, is a key reaction intermediate.

In addition to the mechanistic issues just noted, the sequence of bond dissociation and bond forming steps in reactive collisions of polyatomic ions with surfaces is also of interest although it may be difficult to elucidate. In some cases there is good evidence that SID occurs prior to an ion/surface reaction and the actual reactants responsible for the formation of ion/surface products are the SID fragments; examples are fluorine abstraction by bare transition metal ions generated from metal carbonyls,[18] ions of main group elements formed from corresponding chlorides,[26] carbon radical cations generated from methane ions,[28] and pseudohalogen ions formed from small polyatomic groups.[19] In other cases, there is evidence that dissociation follows or accompanies bond formation; one such example is the formation of $PCl_2F^{+\bullet}$ from the $PCl_3^{+\bullet}$ adduct PCl_3F^+.[27] Because of these complications, it is advantageous to investigate ion/surface reactions with use of monatomic rather than polyatomic ions and this is undertaken in the present study.

Low-energy reactive collisions of monatomic projectile ions at F-SAM surfaces result in the addition of C_mF_n groups to the projectiles. Specific examples are the formation of $^{13}CCF_2^{+\bullet}$ from $^{13}C^{+\bullet}$,[28] WCF_3^+ from $W^{+\bullet}$,[18] and $IC_2F_3^{+\bullet}$ from $I^{+\bullet}$.[27,29] The formation of $IF^{+\bullet}$ and XeF^+ at F-SAM surfaces has also been documented.[28] In a recent study on $Xe^{+\bullet}$ collisions at F-SAM surfaces, the products $XeCF^+$ and $XeCF_2^{+\bullet}$ were observed,[47,48] thus emphasizing the reactive nature of $Xe^{+\bullet}$. It is worth mentioning that at low collision energies (ca. 30−60 eV) xenon cations are often used as chemical sputtering agents, since they readily undergo charge exchange with surface functionalities, allowing them to be ionized and so characterized. Xenon radical cations have therefore been used frequently for the purpose of monitoring surface chemical composition, rather than expressly as reactants for ion/surface reactions.[6,28] Even though reactions of xenon with fluorine[49] and other small organic molecules[50,51] in a gas-phase mixture have been thoroughly studied, the chemical reactivity of xenon radical cations at vacuum/surface interfaces (other than charge exchange) is almost completely unknown. Unlike the better studied but more complex transition metal cations, $Xe^{+\bullet}$ is isoelectronic with neutral iodine and has a simple outer shell electronic structure. In addition, the bonding in XeF^+ has been studied theoretically.[52] Consideration of these factors led to the present investigation.

In parallel to xenon, its nearest neighbors in the periodic table, iodine and krypton, are investigated here too. Earlier work on I^+ with F-SAM surfaces suggested a rich chemistry;[27,29] yet, reactions leading to various products need to be studied in more detail, especially as a function of collision energy. Similarly, $Kr^{+\bullet}$ is of interest but, excluding charge exchange, ion/surface reactions are unknown.[29,53] Reactions of krypton with fluorine[48,51] and methane[54] are known in the gas phase. The current study of the ion/surface reactions of the title ions employs energy resolved mass spectrometry (ERMS) methods.[55] This approach has been widely used in gas-phase CID and ion/molecule studies, as well as in a few SID investigations.[39,54,56] It is also expected that spectra recorded in the threshold energy regime (between 15 and 30 eV lab collision energy) might help to establish qualitatively the energetics of the various reactions, including single fluorine abstraction as well as the abstraction of CF and CF_2 groups. This information can be critical in the elucidation of ion/surface reaction mechanisms by establishing energetic correlations between ion/surface reactions and chemical sputtering.

Theoretical calculations were used to obtain the geometry of some reaction products as well as reaction enthalpies. This information facilitated data interpretation, particularly in cases where the necessary gas-phase thermochemical data were unavailable. Density functional theory (DFT) methods have recently attracted considerable attention and have been applied to many complex organometallic species.[57−59] This method is

(46) Vincenti, M.; Cooks, R. G. *Org. Mass Spectrom.* **1988**, *23*, 317.
(47) Miller, S. A.; Luo, H.; Cooks, R. G.; Pachuta, S. A. *Science* **1997**, *275*, 1447.
(48) Luo, H.; Miller, S. A.; Pachuta, S. J.; Cooks, R. G. *Int. J. Mass Spectrom. Ion Processes* **1997**, *174*, 193.
(49) Berkowitz, J.; Chupka, W. A. *Chem. Phys. Lett.* **1970**, *7*, 447.
(50) Field, F. H.; Franklin, J. L. *J. Am. Chem. Soc.* **1961**, *83*, 4509.
(51) Hovey, J. K.; McMahon, T. B. *J. Am. Chem. Soc.* **1986**, *108*, 528.
(52) MacDougall, P. J.; Schrobilgen, G. J.; Bader, R. F. W. *Inorg. Chem.* **1989**, *28*, 763.
(53) Pradeep, T.; Miller, S. A.; Rohrs, H. W.; Feng, B.; Cooks, R. G. *Mater. Res. Soc. Symp. Proc.* **1995**, *380*, 93.
(54) Field, F. H.; Head, H. N.; Franklin, J. L. *J. Am. Chem. Soc.* **1962**, *84*, 1118.
(55) McLuckey, S. A.; Glish, G. L.; Cooks, R. G. *Int. J. Mass Spectrom. Ion Processes* **1981**, *39*, 219.
(56) Miller, S. A.; Riederer, D. E., Jr.; Cooks, R. G.; Cho, W. R.; Lee, H. W.; Kang, H. *J. Phys. Chem.* **1994**, *98*, 245.
(57) Bauschlicher, C. W., Jr. *Chem. Phys. Lett.* **1995**, *246*, 40.
(58) Thummel, H. T.; Bauschlicher, C. W., Jr. *J. Phys. Chem. A* **1997**, *101*, 1188.

therefore used for the estimation of the reaction thermodynamics in the current study.

Experimental Section

Experiments were performed with a custom-built hybrid mass spectrometer of BEEQ (B = magnetic sector, E = electrostatic analyzer, Q = quadrupole mass analyzer) configuration.[60] Projectile ions were generated in a 70 eV electron impact (EI) ion source and were mass selected and energy focused with the B and E analyzers. Prior to collision, the 2 keV ion beam was decelerated to the desired translational energy with respect to the F-SAM target surface, which was held in a UHV chamber at a nominal pressure of 2×10^{-9} Torr. The nominal laboratory collision energy was calculated as the difference in potential between the ion source and target. The measured potentials have a ±1 eV uncertainty. The ion beam was inclined at 45° with respect to the surface normal while the lens used for extraction of scattered secondary ions was held at 90° with respect to the incoming beam. Scattered product ions were extracted into the post-collision E and Q analyzer system and were mass-analyzed with use of the quadrupole mass filter. To ensure consistency of the data, the flux of the projectile was kept constant, as measured by a moveable Faraday cup located immediately after the BE analyzer section. The surface current was monitored with a Keithley 485 picoammeter. High-purity xenon and krypton gases were obtained from Airco (Murry Hill, NJ), methyl iodide was purchased from Aldrich (Milwakee, WI), and the F-SAM surfaces were made and cleaned in-house, following literature procedures.[11,32,61] In this study, the disulfide $(CF_3(CF_2)_7(CH_2)_2S)_2$ was used to form the self-assembled monolayer by exposure of the gold surface to the solution for 2 weeks.[32] Data are recorded in thomson, where 1 thomson (Th) = 1 dalton per unit charge.[62] At low collision energies (15−30 eV), spectra were collected at 1 eV intervals, while in the 30−70 eV energy range, the collision energy increment was 5 eV. The results were repeated on different days with fresh F-SAM surfaces, and for most peaks in the spectra, only fewer than 20% intensity changes were observed. However, at xenon sputtering energies below 20 eV, intensity variations as large as 50% were observed due to the low signals, especially for low abundance reaction products in their threshold energy region.

Theoretical calculations were first carried out at the Hartree−Fock level for geometry optimization of $XeCF_3^+$, $XeCF_2^{+\bullet}$, $XeCF^+$, XeF^+, ICF_3^+, ICF_2^+, $ICF^{+\bullet}$, $IF^{+\bullet}$, C_3F_8, $C_3F_7^\bullet$, C_2F_6, and $C_2F_5^\bullet$, using the LANL2DZ basis set.[63,64] To treat the effects of electron correlation, all calculations were then repeated by using density functional theory (DFT), with the Becke-3-LYP exchange correlation function.[65,66] Analytical second-derivative calculations were carried out to check for true minima on the potential energy surfaces and corrections for zero-point vibrational energies (ZPVE) were also made. All calculations were carried out with use of the Gaussian 94/DFT program package[67] on IBM RS/6000 RISC workstations at the Purdue University Computing Center.

(59) Holthausen, M. C.; Feidler, A.; Schwarz, H.; Koch, W. *J. Phys. Chem.* **1996**, *100*, 6236.
(60) Winger, B. E.; Laue, H. J.; Horning, S. R.; Julian, R. K., Jr.; Lammert, S. A.; Riederer, D. E., Jr.; Cooks, R. G. *Rev. Sci. Instrum.* **1992**, *63*, 5613.
(61) Chidsey, C. E. D.; Bertozzi, C. R.; Putvinski, T. M.; Mujsce, A. M. *J. Am. Chem. Soc.* **1990**, *112*, 4301.
(62) Cooks, R. G.; Rockwood, A. L. *Rapid Commun. Mass Spectrom.* **1991**, *5*, 93.
(63) Hay, P. J.; Wadt, W. R. *J. Chem. Phys.* **1985**, *82*, 284.
(64) Dunning, T. H., Jr.; Hay, P. J. *Modern Theoretical Chemistry*; Schaefer, H. F., III, Ed.; Plenum: New York, 1976.
(65) Becke, A. D. *J. Chem. Phys.* **1993**, *98*, 1372.
(66) Becke, A. D. *J. Chem. Phys.* **1993**, *98*, 5648.
(67) Frisch, M. J.; Trucks, G. W.; Schlegel, H. B.; Gill, P. M. W.; Johnson, B. G.; Robb, M. A.; Cheeseman, J. R.; Keith, T. A.; Petersson, G. A.; Montgomery, J. A.; Raghavachari, K.; Al-Laham, M. A.; Zakrzewski, V. G.; Ortiz, J. V.; Foresman, J. B.; Cioslowski, J.; Stefanov, B. B.; Nanayakkara, A.; Challacombe, M.; Peng, C. W.; Ayala, P. Y.; Chen, W.; Wong, M. W.; Anfres, J. L.; Replogle, E. S.; Gonperts, R.; Martin, R. L.; Fox, D. J.; Binkley, J. S.; Defrees, D. J.; Baker, J.; Stewart, J. P.; Head-Gordon, M.; Gonzalez, C.; Pople, J. A. *Gaussian 94* (Revision D. 1); Gaussian, Inc.: Pittsburgh, PA, 1995.

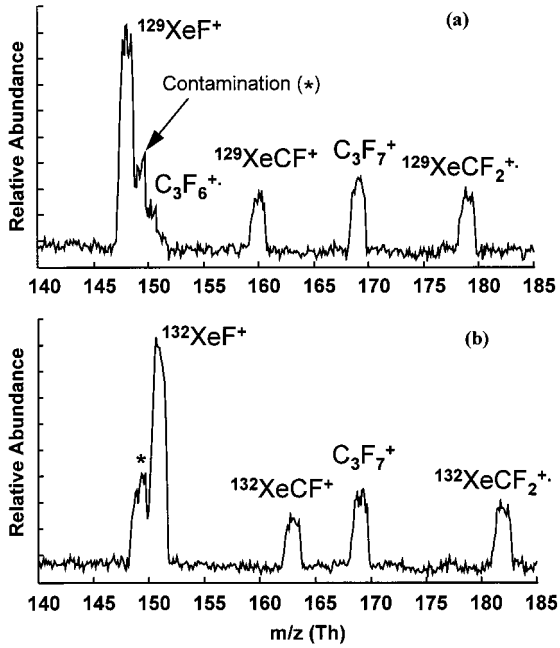

Figure 1. Partial mass spectrum displaying ions released as a result of 55 eV collisions of (a) $^{129}Xe^{+\bullet}$ and (b) $^{132}Xe^{+\bullet}$ at an F-SAM surface.

Results and Discussion

Formation of XeF^+, $XeCF^+$, and $XeCF_2^{+\bullet}$. Figure 1 illustrates the formation of XeF^+, $XeCF^+$, and $XeCF_2^{+\bullet}$ as a result of collisions of xenon projectile ions with an F-SAM surface at 55 eV laboratory collision energy. The spectra indicate clearly the occurrence of two types of processes: chemical sputtering and ion/surface reactions. Both isotopic projectiles, $^{129}Xe^{+\bullet}$ (Figure 1a) and $^{132}Xe^{+\bullet}$ (Figure 1b), yield chemically sputtered products $C_3F_6^{+\bullet}$ (150 Th) and $C_3F_7^+$ (169 Th), as well as a surface contaminant, presumably the ubiquitous phthalate fragment ion (149 Th, labeled *). Also observed, as expected, but not shown in the mass range displayed are other commonly seen chemically sputtered species, such as $CF_2^{+\bullet}$ and CF_3^+, which also arise from ion/surface charge exchange.[6,28] At the same time, the spectra provide evidence for the occurrence of ion/surface reactions which lead to the formation of new bonds, as represented in the scattered ions XeF^+, $XeCF^+$, and $XeCF_2^{+\bullet}$. The relative abundances of XeF^+, (148 Th and 151 Th, in Figure 1, parts a and b, respectively), $XeCF^+$ (160 Th and 163 Th), and $XeCF_2^{+\bullet}$ (179 Th and 182 Th) are identical for the two xenon isotopes. Thus, the products of C−C bond cleavage in the surface, $XeCF^+$ and $XeCF_2^{+\bullet}$, are both unambiguously identified, along with the C−F cleavage product, XeF^+.

Figure 2 shows the relative abundances of the ion/surface reaction products, XeF^+, $XeCF^+$, and $XeCF_2^{+\bullet}$, which are normalized to that for XeF^+ at 35 eV, as a function of laboratory collision energy. All three species are observed in the range of 25 to 80 eV collision energy. Due to the generally low signal for these scattered products (peak heights are about 2 orders of magnitude lower than the CF_3^+ base peak in the scattered ion mass spectra), the signal is noisy. Nevertheless, a common trend is evident: as the collision energy increases, the relative abundances of XeF^+, $XeCF^+$, and $XeCF_2^{+\bullet}$ all increase, reach maxima, and then decrease gradually. Differences in the ERMS data are noticeable for these three species. The broad maxima for XeF^+ and $XeCF_2^{+\bullet}$ lie between 35 and 55 eV, while for $XeCF^+$ the maximum is some 15 eV higher. In the region from ca. 20 to 40 eV, the abundance of XeF^+ shows a sharp rise

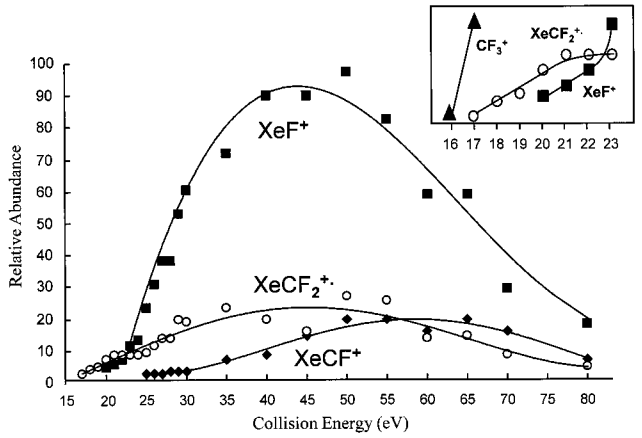

Figure 2. Collision energy dependence of the products XeF^+, $XeCF^+$, and $XeCF_2^{+\bullet}$ scattered from an F-SAM surface upon $Xe^{+\bullet}$ impact.

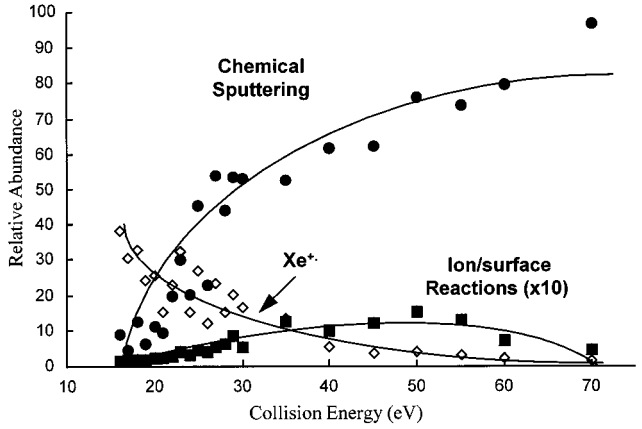

Figure 3. Collision energy dependence of chemical sputtering, $Xe^{+\bullet}$ scattering, and ion/surface reactions. Note that the relative abundance for the ion/surface reactions is shown expanded by a factor of 10.

with collisional energy, while $XeCF_2^{+\bullet}$ and $XeCF^+$ have similar, and relatively small, slopes compared to that of XeF^+. In the very low collision energy regime, $XeCF_2^{+\bullet}$ first appears in the spectra around 17 eV collision energy: this threshold value is a few electronvolts lower than that for XeF^+, which occurs around 20 eV. The threshold collision energy for $XeCF^+$ is considerably higher than that for the other two products, and occurs above 25 eV collision energy.

The chemical sputtering products, including CF^+, $CF_2^{+\bullet}$, CF_3^+, $C_2F_4^{+\bullet}$, $C_2F_5^+$, and $C_3F_5^+$, also show a strong collision energy dependence. The threshold energy for the characteristic CF_3^+ ion at 69 Th is 16 eV, close to the threshold for $XeCF_2^{+\bullet}$, and it is ca. 18 and 27 eV for $C_2F_5^+$ (119 Th) and $C_3F_5^+$ (131 Th), respectively. Charge exchange between the xenon radical cation and the terminal $-CF_3$ and $-C_2F_5$ groups of the F-SAM clearly occurs at very low collision energies, and its collision energy threshold is lower than those for the observed ion/surface reactions. Figure 3 is an ERMS plot that illustrates the collision energy dependence, over a large range, of the three main groups of scattered products: those due to chemical sputtering, ion/surface reactions, and simple scattering of the projectile ion itself. For chemical sputtering, data were recorded by adding the abundances of CF^+, $CF_2^{+\bullet}$, CF_3^+, $C_2F_4^{+\bullet}$, $C_2F_5^+$, and $C_3F_5^+$ at each collision energy (between 16 and 70 eV) and normalizing this total abundance to 100% at 70 eV, at which energy chemical sputtering is the dominant process. The total abundances for the ion/surface reaction products and the scattered $Xe^{+\bullet}$ are simply plotted relative to this value.

Clearly, compared to ion/surface reactions, xenon chemical sputtering of the F-SAM is the dominant process at $Xe^{+\bullet}$ collision energies above 25 eV. The increase in chemical sputtering and the associated increase in projectile ion neutralization (decrease of $Xe^{+\bullet}$ intensity) indicate that charge transfer between $Xe^{+\bullet}$ and F-SAM is increasingly favorable as the projectile ions carry more energy. This is consistent with the fact that this is an endothermic reaction (see below). These observations on the energy dependence of chemical sputtering agree well with recent results on ion/surface reactions with $OCNCO^+$ and $OCNCS^+$.[19] In these cases, the abundance of chemical sputtering products gradually increases with collision energy, while the abundance of the SID products first increases and then decreases at high collision energy due to competing charge exchange and ion/surface reaction processes.[19] Returning to the $Xe^{+\bullet}$ system, one notes that as the collision energy is increased, the excess energy supplied is transferred into internal energy of the chemical sputtering products, generating more fragmentation. In fact, at collision energies above ca. 60 eV, the abundance for CF_3^+, which is the dominant chemical sputtering species at low collision energies, gradually decreases while those of the further fragmentation products, CF^+ and $CF_2^{+\bullet}$, increase rapidly. The observed correlation in the abundances of ion/surface reaction products with those of charge exchange product ions suggests, but does not demand, that charge exchange is involved in the ion/surface reactions at these energies. This issue is considered further below.

Thermochemical Considerations: Formation of XeF^+, $XeCF^+$, and $XeCF_2^{+\bullet}$. Thermochemical data for surface-bound fluorinated compounds are not available; however, estimates can be obtained with use of data for analogous gas-phase reactions. For example, reactions of C_3F_8 can be considered in lieu of those of the F-SAM, as suggested in previous studies.[28,32] Errors are expected to cancel since the change in the target is analogous in gas and surface processes. The gas-phase reaction 1 between $Xe^{+\bullet}$ and C_3F_8 leading to XeF^+ is estimated to be 3.2 eV endothermic and the xenon−fluorine bond energy in XeF^+ is calculated to be 2.0 eV, based on literature values:[30,68]

$$Xe^{+\bullet} + C_3F_8 \rightarrow XeF^+ + C_3F_7^{\bullet} \qquad \Delta H = 3.2 \text{ eV} \quad (1)$$

For reactions leading to the formation of $XeCF^+$ and $XeCF_2^{+\bullet}$, even gas-phase data are unavailable. However, density functional theory (DFT) theoretical calculations show that 0.52 eV is needed to generate $XeCF_2^{+\bullet}$:

$$Xe^{+\bullet} + C_3F_8 \rightarrow XeCF_2^{+\bullet} + C_2F_6 \qquad \Delta H = 0.52 \text{ eV} \quad (2)$$

The observed lower threshold energy for $XeCF_2^{+\bullet}$ formation vs XeF^+ (Figure 2) is consistent with these calculated results. Quantitative interpretation of the collision energy differences is not practical because of the existence of competing fragmentations, the different entropic factors involved, and the quality of the threshold data due to the weak ion signals. However, comparison of the reactions leading to $XeCF_2^{+\bullet}$ and XeF^+ suggests that the former has a tighter activated complex since bond formation in the neutral product is proposed. Such a reaction is not expected to compete favorably with the simpler process leading to XeF^+. This, too, is consistent with the energy resolved data (Figure 2) which show a much more rapid increase of XeF^+ with energy. A more detailed mechanism will be discussed later.

(68) Dymov, B. P.; Skorobogatov, G. A.; Khripun, V. K. *Russ. J. Phys. Chem.* **1991**, *65*, 1107.

A conceivable alternative pathway for forming $XeCF_2^{+\bullet}$ during a collision involves the interaction of a second $Xe^{+\bullet}$ ion with the radical, $C_3F_7^{\bullet}$, generated in reaction 1. The calculated reaction enthalpy is

$$Xe^{+\bullet} + C_3F_7^{\bullet} \rightarrow XeCF_2^{+\bullet} + C_2F_5^{\bullet} \qquad \Delta H = 0.57 \text{ eV} \qquad (3)$$

However, the observations show that $XeCF_2^{+\bullet}$ occurs at a lower threshold energy than XeF^+. Furthermore, the primary ion dose of 0.01% monolayer/second makes the chance for the $C_3F_7^{\bullet}$ radical site at the surface to interact with another xenon ion appear to be negligible, even ignoring the presence of radical scavengers in the vacuum environment. Moreover, if the radical is an intermediate in $XeCF_2^{+\bullet}$ formation, prolonged ion bombardment would leave more radical sites available; thus, the intensity for $XeCF_2^{+\bullet}$ should increase with time at a constant collision energy. For both $XeCF_2^{+\bullet}$ and $XeCF^+$, time and beam flux dependences were not observed. It is therefore concluded that reaction 3 does not contribute significantly to the generation of $XeCF_2^{+\bullet}$.

The third major ion/surface reaction product, $XeCF^+$, may arise in a direct surface process or by gas-phase dissociation of internally excited $XeCF_2^{+\bullet}$ ions. The calculated reaction enthalpy, again using C_3F_8 to represent the surface species, is as follows:

$$Xe^{+\bullet} + C_3F_8 \rightarrow XeCF^+ + C_2F_6 + F^{\bullet} \qquad \Delta H = 3.5 \text{ eV} \quad (4)$$

$$XeCF_2^{+\bullet} \rightarrow XeCF^+ + F^{\bullet} \qquad \Delta H = 3.0 \text{ eV} \qquad (5)$$

Reaction 4 indicates that the direct process requires only slightly more energy than formation of XeF^+ (reaction 1) and $XeCF_2^{+\bullet}$ (reaction 2), but the unimolecular fragmentation (reaction 5) of $XeCF_2^{+\bullet}$ to $XeCF^+$ requires an additional 3.0 eV to induce C−F bond cleavage in $XeCF_2^{+\bullet}$. This additional internal energy can be made available by increasing the original xenon collision energy, leaving the resulting $XeCF_2^{+\bullet}$ product vibrationally excited. Figure 2 shows that there is roughly a 15 eV difference in the maxima of $XeCF_2^{+\bullet}$ and $XeCF^+$, and this shift suggests that at higher collision energy, the ion/surface product $XeCF_2^{+\bullet}$, which presumably has increasingly more internal energy, fragments to $XeCF^+$. It is possible that in the threshold energy region, $XeCF^+$ is formed by direct reaction with the F-SAM.

Note that the shift in the abundance maxima of $XeCF_2^{+\bullet}$ and $XeCF^+$ is about 15 eV and that ΔH for $XeCF_2^{+\bullet}$ fragmentation to $XeCF^+$ is 3.0 eV (reaction 5). Assuming the same 20% translational to internal energy (T → V) conversion factor for these ion/surface reactions as measured for inelastic collisions from SID data,[28,31,32] the two values fit nicely: 20% of 15 eV is 3 eV. (The energy partitioning factor is here applied to the ion/surface reaction product $XeCF_2^{+\bullet}$, rather than the projectile itself as is done in SID.) Much more work will be needed to determine whether this is a representative value.

As shown in the insert to Figures 2 and 3, chemical sputtering occurs at a lower collision energy than the bond-forming ion/surface reactions, indicating that charge exchange must at least be energetically accessible in the collision energy range studied. At low collision energies, only CF_3^+ and $C_2F_5^+$ are observed, suggesting the occurrence of simple C−C bond cleavage of the F-SAM chain after charge exchange with $Xe^{+\bullet}$. Previous studies of hydrocarbon surfaces have also shown that charge exchange is responsible for hydrogen atom abstraction as mentioned in the Introduction. Hence, the ion/surface reaction products, XeF^+ and $XeCF_2^{+\bullet}$, might be formed between neutralized xenon and

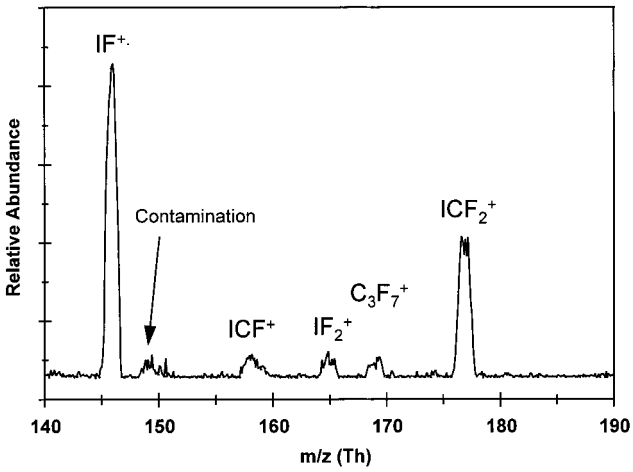

Figure 4. Partial mass spectrum displaying ions released as a result of 40 eV collisions of I^+ at an F-SAM surface.

CF_3^+ in the following ways:

$$Xe + CF_3^+ \rightarrow XeF^+ + CF_2 \qquad \Delta H = 4.7 \text{ eV} \qquad (6)$$

$$Xe + CF_3^+ \rightarrow XeCF_2^{+\bullet} + F^{\bullet} \qquad \Delta H = 4.6 \text{ eV} \qquad (7)$$

$$Xe + C_3F_7^+ \rightarrow XeCF_3^+ + C_2F_4 \qquad \Delta H = 1.1 \text{ eV} \quad (8)$$

As thermochemical data[30] (reaction 6) and DFT calculations (reaction 7) show, these reactions are energetically unfavorable. The initial charge-transfer process is estimated to be further 1.3 eV endothermic (the difference between the ionization energy of CF_3 and the recombination energy of $Xe^{+\bullet}$, 13.4 − 12.1 = 1.3 eV), making the overall reactions considerably less favorable than noncharge exchange processes (reactions 1 and 2) at the same $Xe^{+\bullet}$ collision energy. Reaction of neutral Xe with the other charge exchange products, e.g., $C_3F_7^+$ (reaction 8), could also form the ion/surface reaction products. However, further dissociation of $XeCF_3^+$ to XeF^+ or $XeCF_2^{+\bullet}$ appears to be unfavorable. Even if one allows that the incoming xenon cation could gain some 4 eV (20% of 20 eV at threshold collision energies assuming the translational to internal energy conversion at the F-SAM is 20%),[12,28,31,32] the processes are inaccessible. When allowing for ions generated in the 70 eV EI source with higher than average internal energies and considering the width of the distribution in T → V values, it becomes energetically possible but still unlikely for them to undergo the above endothermic processes. The charge exchange mechanism cannot be ruled out simply on the basis of energetics, but it does seem unlikely.

Comparison with I^+ and $Kr^{+\bullet}$ Reactions. Figure 4 shows the scattered ion mass spectrum of I^+ reaction with the F-SAM surface at a collision energy of 40 eV. Just like $Xe^{+\bullet}$, I^+ reacts readily with the F-SAM surface to form fluorine atom or CF group abstraction products. The relative abundance of the major product ion IF^+ is about 40% of the base peak CF_3^+. It is interesting to note the occurrence of a multiple fluorine atom abstraction product, IF_2^+, which is not observed in the case of $Xe^{+\bullet}$ as the projectile ion. The difference can be attributed to the number of valence electrons available for bond formation. Previous studies showed that W^+ and Si^+, with 5 and 3 valence electrons, respectively, can abstract multiple fluorine atoms to form WF_5^+ and SiF_3^+.[18,27] As expected, the onset of IF_2^+ formation appears at higher collision energy (ca. 30 eV) than

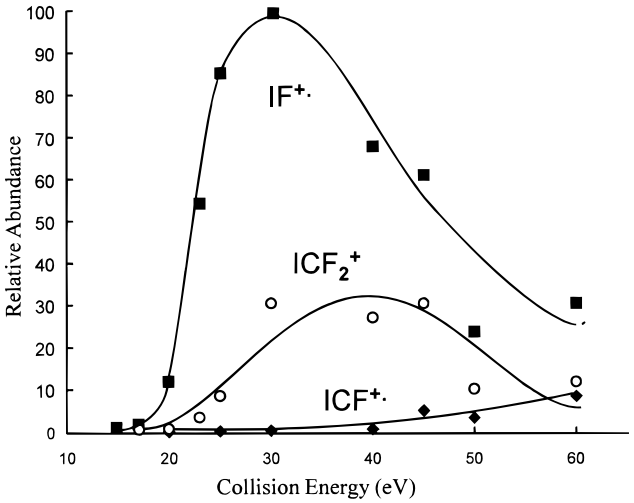

Figure 5. Collision energy dependence of the ion/surface reaction products $IF^{+\bullet}$, $ICF^{+\bullet}$, and ICF_2^+ scattered from an F-SAM surface upon I^+ collision.

that of IF^+, indicating that the process involving multiple C−F cleavage is more endothermic.

Reactions of I^+ with F-SAM surfaces were also studied over a collision energy range of 15−60 eV, the focus being on the formation of the corresponding $IF^{+\bullet}$, $ICF^{+\bullet}$, and ICF_2^+ species. The energy dependence of the relative abundances of these ions is shown in Figure 5, taking $IF^{+\bullet}$ at 30 eV collision energy as 100%. Similarities exist between the behavior of the projectiles $Xe^{+\bullet}$ and I^+: similarly to XeF^+, $IF^{+\bullet}$ is the dominant product and the intensity maxima for $IF^{+\bullet}$ and ICF_2^+ occur at a lower collision energy than that for $ICF^{+\bullet}$. From 15 to 40 eV collision energy, the overall intensity of the ion/surface reaction products is roughly half of that for chemical sputtering by I^+. As the collision energy increases, chemical sputtering becomes dominant as also observed in the xenon case. The thermochemistry calculated by DFT for the corresponding gas-phase reactions is as follows:

$$I^+ + C_3F_8 \rightarrow IF^{+\bullet} + C_3F_7^{\bullet} \qquad \Delta H = 2.5 \text{ eV} \qquad (9)$$

$$I^+ + C_3F_8 \rightarrow ICF_2^+ + C_2F_6 \qquad \Delta H = -0.5 \text{ eV} \qquad (10)$$

$$I^+ + C_3F_8 \rightarrow ICF^{+\bullet} + C_2F_6 + F^{\bullet} \qquad \Delta H = 3.8 \text{ eV} \qquad (11)$$

$$ICF_2^+ \rightarrow ICF^{+\bullet} + F^{\bullet} \qquad \Delta H = 4.4 \text{ eV} \qquad (12)$$

The exothermic reaction 10, which leads to the formation of ICF_2^+, is observed to have a slightly higher threshold energy than that of $IF^{+\bullet}$ (reaction 9). This is in contrast to the corresponding Xe reactions. However, unlike $XeCF_2^{+\bullet}$, ICF_2^+ is a closed-shell species, and a barrier along the reaction coordinate associated with the formation of closed-shell products may be assumed. Chemical sputtering of CF_3^+ by I^+ has a threshold as low as 15 eV collision energy, at which energy only $IF^{+\bullet}$ is observed, and the predominant scattered ion is the reflected I^+ ion.

When considering the charge exchange route, neutralization of I^+ at an F-SAM surface is 2.9 eV endothermic (the difference between the ionization energy of CF_3 and the recombination energy of I^+, 13.4 − 10.5 = 2.9 eV), and the subsequent reaction enthalpies are as follows:

$$I^{\bullet} + CF_3^+ \rightarrow IF^{+\bullet} + CF_2 \qquad \Delta H = 2.3 \text{ eV} \qquad (13)$$

$$I^{\bullet} + CF_3^+ \rightarrow ICF_2^+ + F^{\bullet} \qquad \Delta H = 1.8 \text{ eV} \qquad (14)$$

Once again, these reactions are energetically unfavorable as thermochemical data[30] (reaction 13) and DFT calculation (reaction 14) show, when compared to noncharge exchange processes.

The intact C−C cleavage product, $ICF_3^{+\bullet}$, occurs in the collision energy range 17 to 45 eV, although its abundance is very low. The $ICF_3^{+\bullet}$ ion appears to be stable to dissociation only at relatively low energies compared to the other reaction products. The energetics of its formation and dissociation are shown in reactions 15 and 16. The absence of the corresponding methylated xenon ion is easily explained in light of the calculated thermochemistry, which shows that it dissociates even more readily (reaction 17):

$$I^+ + C_3F_8 \rightarrow ICF_3^{+\bullet} + C_2F_5^{\bullet} \qquad \Delta H = 1.7 \text{ eV} \qquad (15)$$

$$ICF_3^{+\bullet} \rightarrow CF_3^+ + I^{\bullet} \qquad \Delta H = 1.4 \text{ eV} \qquad (16)$$

$$XeCF_3^+ \rightarrow CF_3^+ + Xe \qquad \Delta H = 0.5 \text{ eV} \qquad (17)$$

The minimum 1.4 eV requirement for the fragmentation of $ICF_3^{+\bullet}$ allows it to be observed with low abundance, but the less stable $XeCF_3^+$ is not detected. Note that a related ion, $XeCH_3^+$, was observed in a previous gas-phase study.[53]

Like I^+, Br^+ ions showed $BrF^{+\bullet}$, $BrCF^{+\bullet}$, and $BrCF_2^+$ reaction products upon collision with F-SAM surfaces.[27] No reactions of ionized krypton were observed at any collision energy studied, only chemical sputtering of the F-SAM occurred, and $Kr^{+\bullet}$ was observed as a scattered ion. The absence of krypton ions in the scattered ion mass spectra, also found in earlier studies,[29,52] indicates that virtually all $Kr^{+\bullet}$ ions are neutralized as a result of ion/surface collisions, a result that is consistent with the near resonance of electron transfer to the F-SAM surface. Charge exchange for either I^+ or Br^+ (recombination energy is 11.8 eV)[35] is less favorable than that for $Kr^{+\bullet}$.

Theoretical calculations of the structures of the observed ion/surface reaction products are presented in Figure 6. For Xe or I containing species, Hartree−Fock geometry optimization with the LANL2DZ basis set fails to give reasonable bond lengths and bond angles. The Becke-3-LYP density functional method was therefore used to optimize the ion structures. The calculated Xe−F^+ bond length of 2.006 Å is close to the value of 1.947 Å, reported in a previous calculation.[69] The positive charge in $XeCF^+$ and $XeCF_2^{+\bullet}$ is almost equally shared between xenon and carbon, while for the ICF_n^+ ($n = 1-3$) species iodine retains at least 75% of the charge.

$Xe^{+\bullet}$ Reaction Mechanisms. (1) C−F Bond Cleavage and Formation of XeF^+. The net endothermicity of breaking a C−F bond and forming a Xe−F bond is roughly 3 eV, as shown in reaction 1. Scheme 1 illustrates four possible reaction pathways which might lead to XeF^+ in the course of ion/surface collisions.

In route 1, the xenon radical cation binds to a fluorine atom at the surface, generating a fluoronium ion intermediate. Subsequent cleavage of the bond between fluorine and carbon yields XeF^+. This endothermic reaction appears to require the

(69) Tanaka, S.; Sugimoto, M.; Takashima, H.; Hada, M.; Nakatsuji, H. *Bull. Chem. Soc. Jpn.* **1996**, *69*, 953.

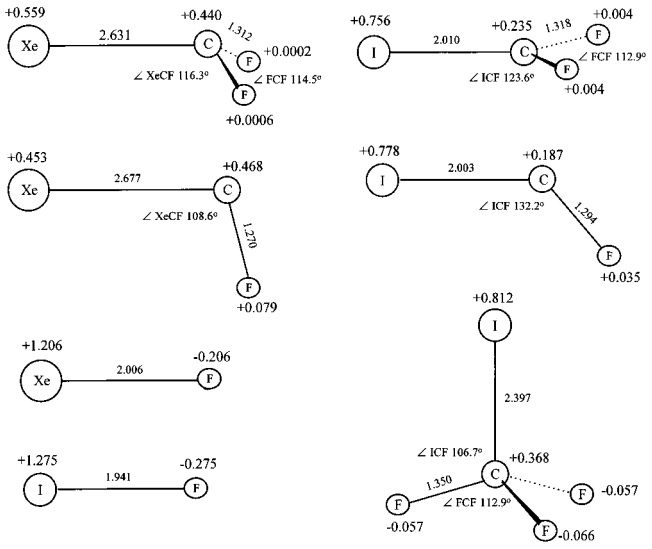

Figure 6. Calculated DFT geometries for XeF^+, $XeCF^+$, $XeCF_2^{+\bullet}$, $IF^{+\bullet}$, $ICF^{+\bullet}$, ICF_2^+, and $ICF_3^{+\bullet}$. Bond lengths are in Å; Mulliken charges are labeled at each atom.

Scheme 1. Possible Mechanisms for the Formation of XeF^+ in Collisions with an F-SAM Surface[a]

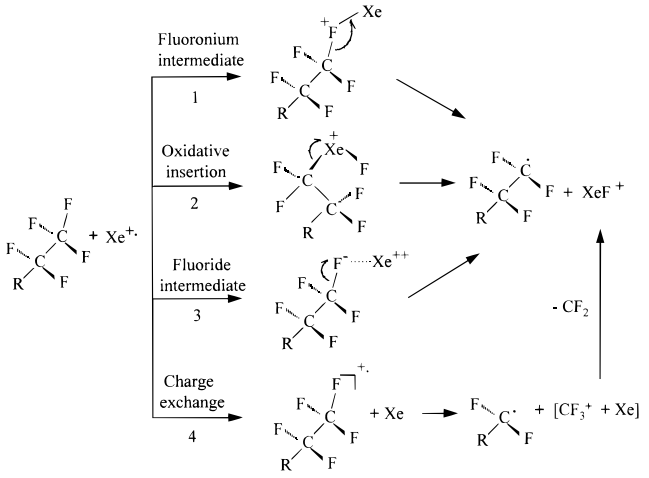

[a] Route 1 involves a fluoronium ion intermediate, route 2 involves oxidative insertion, route 3 involves fluoride intermediate, and route 4 involves charge exchange.

smallest entropy change and so might be favored under high energy conditions. It was proposed earlier that fluoronium ion intermediates are involved in ion fluorine atom abstraction by metal ions from F-SAM surfaces,[18] and in the pickup of fluorine atoms from F-SAM surfaces by methane-derived projectile ions such as CH_3^+.[28] Transhalogenation between the incoming Cl-, Br-, and I-containing ions and the F-SAM surface,[6] and exchange reactions involving NCO and NCS groups and fluorine atoms at F-SAM surfaces may also occur by this mechanism, which involves formal electron donation from the highly electronegative fluorine atom.[19]

In route 2, xenon is oxidatively inserted into the C−F bond, whereupon cleavage of the weak Xe−C bond results in identical products to those which occur in route 1. The surface reaction intermediate is a xenonium ion and may be quite unstable since the Xe−F and Xe−C bonds are both weak. Oxidative insertion of $Fe^{+\bullet}$ into the C−F bond in fluorobenzene has been reported in gas-phase experiments.[70,71] In these studies, loss of HF was observed due to the strong H−F bonding and the stability of the Fe−C_6H_4 bond, estimated to be 3.6 eV.[71] In comparison, the Xe−C bond in $XeCF_2^{+\bullet}$ is calculated to be only 1.4 eV while an experimental value for the Xe−C bond in $XeCH_3^+$, as mentioned earlier, is 2 eV.[51] This reaction pathway is thus energetically less demanding than route 1 and may be the dominant process at very low collision energies. Initial coordination of the ion at fluorine[72] may be involved in route 2.

In route 3, an electron is transferred from $Xe^{+\bullet}$ to the fluorocarbon chain to form a fluoride intermediate, $[Xe^{2+}\cdots {}^-FCF_2-R]$, formally a xenon dication complexed to a negatively charged fluoride anion. Cleavage of the F^-−C bond leads to the formation of XeF^+. Recently, Schwarz and co-workers have proposed that C−F bond cleavage in gas-phase ionic reactions can proceed by a similar fluoride mechanism.[72] Their experimental and theoretical evidence suggest that the reaction of lanthanide with fluorocarbons involves charge exchange formally to give a metal dication and a fluoride anion. Charge exchange occurs from the metal ion M^+ to the fluorine, followed by cleavage of the C−F bond and the formation of the MF^+ species. The high reactivity of the lanthanide cations with fluorocarbons appears to be a simple consequence of the very low second ionization energy of the metal ions, which are in the range of 10−12 eV, e.g. La^+ (IE = 5.6 eV) to $La^{2+\bullet}$ (IE = 11.1 eV) requires only 5.5 eV. A mechanism of this type has also been shown to apply to CaF^+ formation from $Ca^{+\bullet}$, a conclusion supported by high-level calculations.[73] Considering that xenon has a very high second ionization energy (21.2 eV), even when allowing for the high electron affinity of the fluorine atom (EA = 3.5 eV), the formation of XeF^+ via $[Xe^{2+}\cdots F^-CF_2-R]$ would require 17.7 eV to drive the reaction. Note that for calcium (second IE = 11.9 eV), the corresponding value is lower by 9.3 eV, which is the difference between their second IEs. The difference in energetics is striking. Thus, this pathway is believed to be energetically unfavorable and the least probable mechanism of C−F cleavage for the projectiles employed in these low-energy ion/surface collisions.

In the fourth route, the incoming $Xe^{+\bullet}$ undergoes charge exchange with the fluorocarbon, producing a surface-bound radical cation. In a process which is similar to that involved in the reactions of hydrocarbon radical cations with hydrocarbon surfaces,[11,24,33,41] the fragments of dissociation of the surface-bound cation, including CF_3^+, then react with the now-neutralized xenon to form XeF^+ with expulsion of CF_2 neutral. This process requires more energy than the processes in routes 1 and 2 that do not require charge exchange [compare reactions 1 and 6], since $Xe^{+\bullet}$ must first charge exchange with the surface (1.3 eV endothermic) and then react to form XeF^+ (an additional 4.7 eV endothermic (reaction 6)), making the overall process 6 eV endothermic. The XeF^+ threshold collision energy is 20 eV, barely enough for this reaction to occur through this route. Morever, the formation of $XeCF^+$ from $Xe^{+\bullet}$ requires a total of only 3.5 eV (reaction 4) and its threshold collision energy is at 25 eV. If charge exchange is responsible for XeF^+ formation, considering the energetics, its threshold collision energy should be higher than that for $XeCF^+$. But the reverse is observed. Furthermore, consider as already noted that the recombination energy of $Kr^{+\bullet}$ is 14 eV, its neutralization at the surface (IE estimated at 13.4 eV) is a resonance process and exothermic by 0.6 eV. Krypton neutralization was observed at all energies

(70) Dietz, T. G.; Chatellier, D. S.; Ridge, D. P. *J. Am. Chem. Soc.* **1978**, *100*, 4905.
(71) Bjarnason, A.; Taylor, J. W. *Organometallics* **1989**, *8*, 2020.
(72) Cornehl, H. H.; Hornung, G.; Schwarz, H. *J. Am. Chem. Soc.* **1996**, *118*, 9960.
(73) Harvey, J. N.; Schroder, D.; Koch, W.; Danovich, D.; Shaik, S.; Schwarz, H. *Chem. Phys. Lett.* **1997**, *278*, 391.

Scheme 2. Possible Mechanisms for the Formation of $XeCF_2^{+\bullet}$ in Collisions with an F-SAM Surface[a]

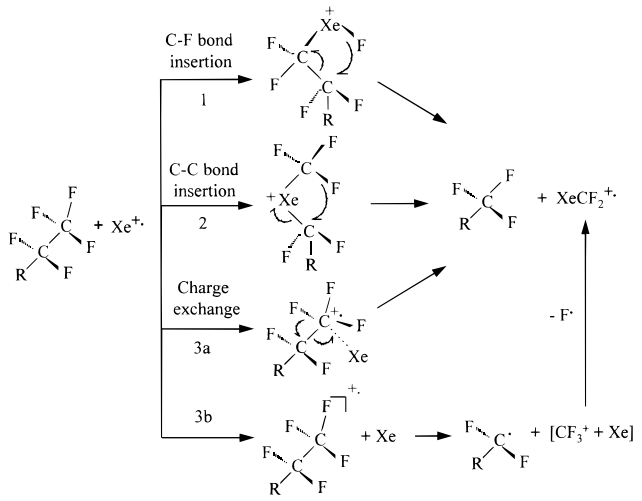

[a] Route 1 involves oxidative insertion of the C−F bond, route 2 involves oxidative insertion of the C−C bond, and routes 3a and 3b involve charge exchange followed by reaction.

without yielding any ion/surface reaction products. The Kr−F^+ and Kr−C^+ (in $KrCH_3^+$) bonds are not weak (1.6 eV[48] and 0.9 eV[74]) compared to the bonds in the corresponding xenon species which were observed over a wide collision energy range. The absence of krypton reaction products is also consistent with the suggestion that charge exchange, a favorable process for $Kr^{+\bullet}$, is not essential for fluorine abstraction ion/surface reactions to occur. (One recognizes that other factors, such as polarizability, may limit the reactivity of kryton.) The above analysis strongly indicates that charge exchange does not play a significant role in forming the ion/surface reaction products observed in this study.

(2) C−C Bond Cleavage and Formation of $XeCF_2^+$. The thermochemical requirement for generating $XeCF_2^+$ in the gas-phase reaction between $Xe^{+\bullet}$ and C_3F_8 is ca. +0.5 eV (reaction 2), i.e., it is slightly endothermic. But this process is energetically more favorable than XeF^+ formation. As shown in Figure 2, $XeCF_2^{+\bullet}$ has the lowest collision energy threshold of the various ion/surface reactions. Scheme 2 illustrates four possible pathways which might lead to $XeCF_2^+$ formation.

In route 1, oxidative insertion of $Xe^{+\bullet}$ into the C−F bond followed by homolytic C−C bond cleavage generates the products $XeCF_2^{+\bullet}$ and a neutral surface-bound fluorocarbon. This is similar to the proposed oxidative insertion mechanism for XeF^+ formation (Scheme 1, route 2), the difference lying in the proposed fluorine atom migration and C−C bond, instead of C−Xe bond cleavage. The formation of a strong C−F bond while breaking weak C−C and Xe−F bonds is energetically favorable, even though entropically demanding. At higher energies a neutral fluorine atom is probably lost after oxidative insertion without forming the new C−F bond at the β carbon. In this case, homolytic C−C bond cleavage again generates $XeCF_2^{+\bullet}$ but also a surface-bound radical, and the energy requirements rise correspondingly.

In route 2, xenon is oxidatively inserted into the C−C bond and fluorine migration followed by, or concerted with, C_β−Xe bond cleavage generates the same final products as route 1. Ion insertion into C−C bonds has been observed in ion beam experiments with bare transition metals, such as Co^+.[75,76] It is known from these studies that oxidative addition can be a low-energy process[74] and prior neighboring C−H bond activation is not necessarily required. It is therefore expected that $Xe^{+\bullet}$ will insert into the first C−C bond of the SAM chain, especially at low collision energies, and that this process will be competitive with the xenon C−F bond insertion pathway. Both reactions lead to the same products by F migration and neutral fluorine atom loss without new C−F bond formation may be a high-energy variant of both processes. It is worth pointing out that C_α−Xe bond cleavage in the insertion product yields CF_3^+. Based simply on the observation of CF_3^+ ions, this process is indistinguishable from chemical sputtering.

Route 3 considers charge exchange between $Xe^{+\bullet}$ and the surface CF_3 group. The neutralized xenon may be loosely bound to the charged terminal CF_3^+ group through ion-induced dipole interactions favored by its high polarizibility. Subsequent 1,2-fluorine migration and Xe−C bond formation lead to the final products (route 3a). The similarity of threshold energies for $XeCF_2^{+\bullet}$ (17 eV) and chemically sputtered CF_3^+ (16 eV) shows that this mechanism is energetically accessible, as discussed earlier. Similarly to routes 1 and 2, route 3a is a low-energy process due to the formation of a new C−F bond, while a higher energy version (route 3b) in which no new C−F bond is formed may also occur. As in route 4, Scheme 1, Xe and CF_3^+ recombine in an ion/molecule reaction fashion (route 3b) to generate the final product $XeCF_2^{+\bullet}$ with the loss of a fluorine atom, an endothermic process comparable to XeF^+ formation in the same fashion. However, this possible process is not considered favorable for reasons explained earlier.

The reaction generating XeF^+ and $XeCF_2^{+\bullet}$ may also proceed via formation of $XeCF_3^+$, which subsequently fragments to generate these species. Although $XeCF_3^+$ was not observed, its low dissociation energy (see above) makes it impossible to exclude this possibility.

I^+ Reaction Mechanisms. Oxidative insertion may also be responsible for the formation of $ICF_3^{+\bullet}$ since an electronically more stable F−I^+−C (I^+ has six outer shell electrons) group may undergo homolytic C−C bond cleavage, leading to the observed product $ICF_3^{+\bullet}$. Iodine has a lower recombination energy (RE = 10.5 eV) than xenon and chemical sputtering is not as facile. The abundance of chemically sputtered CF_3^+ ions is typically only a factor of 2 greater than that of $IF^{+\bullet}$ ions, the major ion/surface reaction product, when I^+ is the projectile ion. However, chemical sputtering is still evident at $IF^{+\bullet}$ threshold energies, which indicates that charge exchange does occur. If $IF^{+\bullet}$ and ICF_2^+ are generated after I^+ charge exchange with the surface, ICF_2^+ ions are expected to be observed first since this reaction is less endothermic than $IF^{+\bullet}$ formation (reactions 13 and 14). But the opposite was observed. This again suggests that charge exchange does not contribute to the generation of ion/surface reaction products. The lowest threshold charge exchange product, CF_3^+, was first observed at virtually identical projectile collision energies for $Xe^{+\bullet}$ and I^+, but the subsequent reaction leading to XeF^+ (reaction 6) is 2.4 eV more endothermic than that leading to $IF^{+\bullet}$ (reaction 13). However, there is only a 5 eV difference in the observed threshold collision energies, a value which is inconsistent with the T → V partitioning data already cited. These considerations once more indicate that charge exchange is unlikely to be responsible for ion/surface reactions in the current study.

The two-step reactive scattering model proposed by Kang and co-workers[23] is worth mentioning here. In their study, low-energy collisions of Cs^+ ion with H_2O-adsorbed Si(111) surface

(74) Holtz, D.; Beauchamp, J. L. *Science* **1971**, *173*, 1237.
(75) Armentrout, P. B.; Beauchamp, J. L. *J. Am. Chem. Soc.* **1980**, *102*, 1736.
(76) Karrass, S.; Schwarz, H. *Organometallics* **1990**, *9*, 2034.

lead to observation of $Cs(H_2O)^+$, $Cs(OH)^+$, $Cs(SiO)^+$, and $CsSi^+$. It was proposed that the reactive scattering process involves the physical desorption of neutral adsorbates due to ion/surface collisions, and subsequent association reaction of Cs^+ and the desorbed neutrals. Both OH and H_2O are believed to be present on the surface and to be desorbed during the collision in their origin state. We suggest that the formation of fluorine atom or CF_x group ($x = 1-3$) abstraction products by $Xe^{+\bullet}$ and I^+ ions does not follow this two-step model. The similarity of energy dependence of product ion abundances suggests that the reactions proceed via a similar mechanism for $Xe^{+\bullet}$ and I^+. The observation of the multiple F-atom abstraction product, IF_2^+, appears not to support the post-collision gas-phase association reaction mechanism, which requires many-body collisions to proceed. The formation of IF_2^+ is consistent with our previous results of multiple F-atom pick-up reactions by atomic and polyatomic ions, in which the maximum number of F atoms that can be added to the projectile depends on the availability of valence electrons, and the abstraction reactions occur at the surface.

Conclusion

Products of C−C and C−F cleavage in self-assembled fluorcarbon monolayers ($XeCF_2^{+\bullet}$ and $XeCF^+$, along with XeF^+) are generated during collisions of $Xe^{+\bullet}$ over a wide collision energy range (15−80 eV). A comparable study with I^+ shows that its behavior is similar to $Xe^{+\bullet}$ in terms of the generation and the collision energy dependence of $IF^{+\bullet}$, $ICF^{+\bullet}$, and ICF_2^+ species, but that the intact C−C cleavage adduct, $ICF_3^{+\bullet}$, as well as the multiple F-atom abstraction product, IF_2^+, are also observed. Threshold energy measurements for each ion/surface reaction product indicate that $XeCF_2^{+\bullet}$ is formed at the lowest laboratory collision energy, ca. 17 eV, consistent with the estimated thermochemistry which suggests its reaction enthalpy is lowest among the three. The three products are formed directly from ion/surface collisions at undamaged terminal groups of the fluorinated alkylthiolate chain. Fragmentation of $XeCF_2^{+\bullet}$ contributes to the abundance of $XeCF^+$ at high collision energies, when the $XeCF_2^{+\bullet}$ ions formed have excess internal energy available for further fragmentation. Chemical sputtering of F-SAM surfaces by $Xe^{+\bullet}$ and I^+ occurs at the lowest collision energy investigated, suggesting that charge exchange has a lower threshold than ion/surface reactions for both projectiles, and it is also the dominant process for $Xe^{+\bullet}$ at all collision energies.

Several reaction pathways are discussed in the light of calculated reaction enthalpies, previous thermochemical data, and the experimental observations. These results indicate that for C−F bond activation leading to XeF^+, a fluoronium intermediate is favored at high collision energies and that oxidative insertion is the favored pathway at low energy. Oxidative insertion appears also to lead to C−C cleavage. The ion/surface reactions leading to $XeCF_2^+$ occur with T → V partitioning efficiency which is similar to that for SID processes at F-SAM surfaces. Although charge exchange is energetically accessible at all collision energies, it appears that it does not contribute to the ion/surface reactions investigated. This is also consistent with previous studies of metal and nonmetal ions on F-SAM surfaces,[18,27,28] where experimental observations indicate that charge exchange is often not involved in ion/surface reactions.

Acknowledgment. This work was supported by the National Science Foundation (CHE-9223791 and 9732670). V.G. thanks the Fonds zuer Foerderung der Wissenschaftlichen Forschung (FWF), Austria, for fellowship support.

JA973201K